Vol. 192, No. 3, 1993 BIOCHEMICAL AND BIOPHYSICAL RESEARCH COMMUNICATIONS
May 14, 1993 Pages 1238-1244

THREE-DIMENSIONAL STRUCTURE OF ω-CONOTOXIN GVIA DETERMINED BY ^{1}H NMR

P. Sevilla[1], M. Bruix[2], J. Santoro[2], F. Gago[3], A.G. García[4], and M. Rico[2]

[1] Dpto. Química Física II, Facultad de Farmacia, Instituto Pluridisciplinar, Universidad Complutense, 28040 Madrid, Spain

[2] Instituto de Estructura de la Materia, CSIC, Serrano 119, 28006 Madrid, Spain

[3] Dpto. Fisiología y Farmacología, Campus Universitario, 28871 Alcalá de Henares, Madrid, Spain

[4] Dpto. Farmacología, Facultad de Medicina, Universidad Autónoma, 28029 Madrid, Spain

Received March 31, 1993

SUMMARY: ω-Conotoxin GVIA, a peptide of 27 amino acid residues and three disulfide bridges, has been studied by NMR techniques. The complete assignment of the corresponding proton NMR spectra was performed by two-dimensional sequence specific methods at 288 K and pH 3.5. On the basis of 169 distance restraints derived from this analysis, the three-dimensional structure was obtained. A total of 30 initial structures were generated by distance geometry methods and further refined by restrained energy minimization techniques yielding a final set of 8 structures. The mean root-mean-square deviation between each of the 8 structures and the mean atomic coordinates for all residues is 0.82±0.06 Å for the backbone atoms and 1.45±0.18 Å for all non-H atoms. The structure shows a globular folding pattern that is stabilized by the three disulfide linkages and a number of intramolecular hydrogen bonds. A total of 14 hydroxyl groups are found at the periphery fully exposed to the solvent. These groups, together with the charged side chains of Lys and Arg residues emerging radially from the peptide core, provide specific recognition elements for the interaction of this toxin with neuronal calcium channels.

The venoms from marine snails of the genus *Conus* are emerging as one of the great treasure houses of neuropharmacological agents. The biologically active substances are small peptides, most of them multiply disulfide-bonded, which block different neurotransmitter receptors and ion channels (1,2). ω-Conotoxin GVIA (ω-CgTx) from *C. geographus* and *C. magus* consists of 27 amino acid residues constrained by three disulfide bridges. It reduces neurotransmitter release by interfering with Ca^{2+} entry into the nerve terminal during the presynaptic action potential (3) and is proving to be a valuable research tool for the characterization and classification of voltage-sensitive Ca^{2+} channels in mammalian cells (4).

The common structural feature in most *Conus* peptides is the pattern of Cys residues, which can be arranged in three major frameworks : CC---C---C (α-conotoxins), CC---C---C---CC (μ-conotoxins), and C---C---CC---C---C (ω-conotoxins). The wide range of pharmacological actions, even within the same family of peptides, originates from the hypervariability of the loop regions between the Cys residues (2).

Abbreviations: ω-CgTx, ω-Conotoxin GVIA; TSP, sodium 3-trimethylsilyl-(2,2,3,3,-$^2H_4$)propionate; COSY, 2D correlated spectroscopy; HOHAHA, homonuclear Hartmann-Hahn spectroscopy; NOESY, 2D nuclear Overhauser enhancement spectroscopy; NOE, nuclear Overhauser enhancement; RMSD, root-mean-square deviation.

0006-291X/93 $4.00

A first step towards a better understanding of the molecular determinants of binding specificity in this class of compounds is the elucidation of their tertiary structure. To date this information is only available for α-conotoxin GI (5,6) and μ-conotoxin GIIIA (7,8). The present study focuses on the three dimensional structure of ω-CgTx which has been elucidated in aqueous solution by 2D ^1H nuclear magnetic resonance (NMR) techniques, and variable target function and energy minimization algorithms.

MATERIALS AND METHODS

ω-CgTx was obtained directly from SIGMA, with 99% purity. The sample was prepared by dissolving 2 mg of protein into 0.5 ml of either D_2O or 90% H_2O/10% D_2O, and adjusting the pH to 3.5. COSY (9), HOHAHA (10), and NOESY (11) experiments with mixing times of 250 ms and 150 ms in the H_2O samples and 150 ms in the D_2O sample were performed. NMR spectra were recorded on a Bruker AMX-600 spectrometer operating at 600 MHz, and phase-sensitive time-proportional phase incrementation was used in all cases. The temperature was set at 288 K and 308 K. TSP was used as the internal reference. In all cases preirradiation was used for water resonance suppression. Spectra were recorded with 512 (t_1) and 2048 (t_2) data points. Zero filling in the t_1 dimension and phase-shifted squared sine-bell functions were applied before Fourier transformation.

Proton resonance assignments were obtained semiautomatically using the TRITON package (12); manual assignment was used to complete the ^1H chemical shift table and to assign additional NOESY cross-peaks. Upper distance restraints were obtained from the peak volumes, adjusting the $C^{\beta}H$-$C^{\beta}H$ distances to 1.9 Å. Pseudoatom corrections (13) were used to define distances when protons in aromatic rings and methyl and methylene groups were involved.

Using the unambiguous connectivities initially detected, trial structures were obtained by using a variable target function algorithm as implemented in the DIANA program (14). The best of these preliminary structures were used to assign the remaining cross peaks in the NOESY spectra, thus providing a refined input restraint data set for a new DIANA run. The whole process was repeated several times until no additional cross-peaks were assigned. This way all the peaks were identified, and a final list of proton-proton distance restraints was obtained.

New structures were then constructed by applying these distance restraints to a set of initial conformations generated by using random dihedral angle values for the peptide backbone. These structures were used within the GLOMSA program (14) to obtain stereospecific assignments. Among the resulting solutions, those conformers with the smaller final target function values were selected to represent the structure of the peptide in solution. These were subjected to restrained energy minimization using the GROMOS (15) suite of programs and a square-well potential for the NOE empirical energy term with a force constant of 40 kJ mol^{-1} $Å^{-2}$. By averaging the least squares fitted coordinates of the eight conformers which better satisfied the restraints, a mean atomic structure was obtained which was energy-minimized as before. Pairwise comparisons between the final structures were made by calculating the respective root-mean-square deviations (RMSD) (16).

RESULTS

Using COSY and HOHAHA spectra at 288 K the different amino acid spin systems were identified with the exception of three $C^{\alpha}H$ protons whose resonances overlapped with water. In order to obtain these resonances, HOHAHA analysis at 308 K was necessary. Patterns of Lysines, Arginines and Hydroxyprolines were easily identified in the HOHAHA spectra. Complete sequential assignment was carried out on the basis of NOESY data and well established procedures (17). Figure 1 shows the sequential connectivities derived from NOESY cross peaks. A complete resonance assignment including the C terminal amide protons was obtained. Table 1 lists the ^1H chemical shifts for all protons of ω-CgTx.

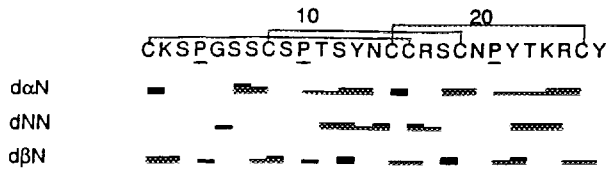

Figure 1. Amino acid sequence of ω-CgTx and sequential assignments. Sequential connectivities (dαN, dNN, dβN), manifested by strong (d < 2.5 Å), intermediate (2.5 Å < d < 3.5 Å), and weak (d > 3.5 Å) NOESY cross peaks are represented by thick, standard, and thin lines, respectively. P in the sequence means 4-hydroxyproline.

A total of 247 unambiguous NOESY cross correlations were identified leading to a list of 169 relevant distance restraints. Figure 2 shows the distribution of the observed NOE connectivities. By use of the DIANA program, 500 random starting structures yielded a total of 30 structures, which were used

Table 1. ^{1}H chemical shift (ppm) of ω-conotoxin GVIA at 288 K and pH 3.5

Residue	NH	$C^{\alpha}H$	$C^{\beta}H$	Others
1 Cys		4.57	3.24 3.04	
2 Lys	9.45	4.64	1.92 1.87	$C^{\gamma}H$ 1.52 1.43 $C^{\delta}H$ 1.70 1.66 $C^{\varepsilon}H$ 3.02 3.02 $N^{\zeta}H$ 7.53
3 Ser	9.01	4.54	4.01 3.64	
4 Hyp	--	4.22	2.11* 2.44*	$C^{\gamma}H$ 4.73 $C^{\delta}H$ 3.85 3.85
5 Gly	9.28	4.53 3.67		
6 Ser	7.72	4.50	3.94 3.84	
7 Ser	8.93	4.73	3.90 3.90	
8 Cys	8.39	4.98[a]	3.07* 2.95*	
9 Ser	8.42	4.95[a]	4.00 3.72	
10 Hyp	--	4.44	2.08* 2.37*	$C^{\gamma}H$ 4.56 $C^{\delta}H$ 4.03 4.03
11 Thr	7.63	4.10	4.48	$C^{\gamma}H_3$ 1.14
12 Ser	7.51	4.39	3.85 3.85	
13 Tyr	8.13	4.52	3.27 2.93	$C^{\delta}H$ 7.08 $C^{\varepsilon}H$ 6.84
14 Asn	8.30	4.87	3.02 2.74	$N^{\delta}H_2$ 7.59 7.05
15 Cys	8.75	4.66	2.46* 3.00*	
16 Cys	9.50	4.56	2.79 3.26	
17 Arg	8.40	4.61	2.04 1.70	$C^{\gamma}H$ 1.54 1.54 $C^{\delta}H$ 3.19 3.19 $N^{\varepsilon}H$ 7.21
18 Ser	7.21	4.61	4.04 4.04	
19 Cys	8.90	4.79	2.95 2.80	
20 Asn	7.93	4.54	1.27* 3.47*	$N^{\delta}H_2$ 7.49 6.79
21 Hyp	--	4.31	1.70* 2.24*	$C^{\gamma}H$ 4.51 $C^{\delta}H$ 3.92 3.92
22 Tyr	8.34	4.39	3.15 3.15	$C^{\delta}H$ 7.28 $C^{\varepsilon}H$ 6.90
23 Thr	7.08	4.23	4.23	$C^{\gamma}H_3$ 1.16
24 Lys	8.57	3.63	2.37 2.06	$C^{\gamma}H$ 1.31 1.31 $C^{\delta}H$ 1.70 1.66 $C^{\varepsilon}H$ 3.02 3.02 $N^{\zeta}H$ 7.58
25 Arg	7.33	5.24	1.47 1.29	$C^{\gamma}H$ 1.63 1.39 $C^{\delta}H$ 3.14 3.08 $N^{\varepsilon}H$ 7.19
26 Cys	9.26	4.95[a]	2.80* 3.66*	
27 Tyr	9.32	4.46	2.87* 3.18*	$C^{\delta}H$ 7.30 $C^{\varepsilon}H$ 7.06 CONHZ 7.63* CONHE 8.26*

* indicates that $C^{\beta}H$ are stereospecifically assigned. $C^{\beta}H2$ is the first one, $C^{\beta}H3$ the second one.
[a] measured at 308 K.

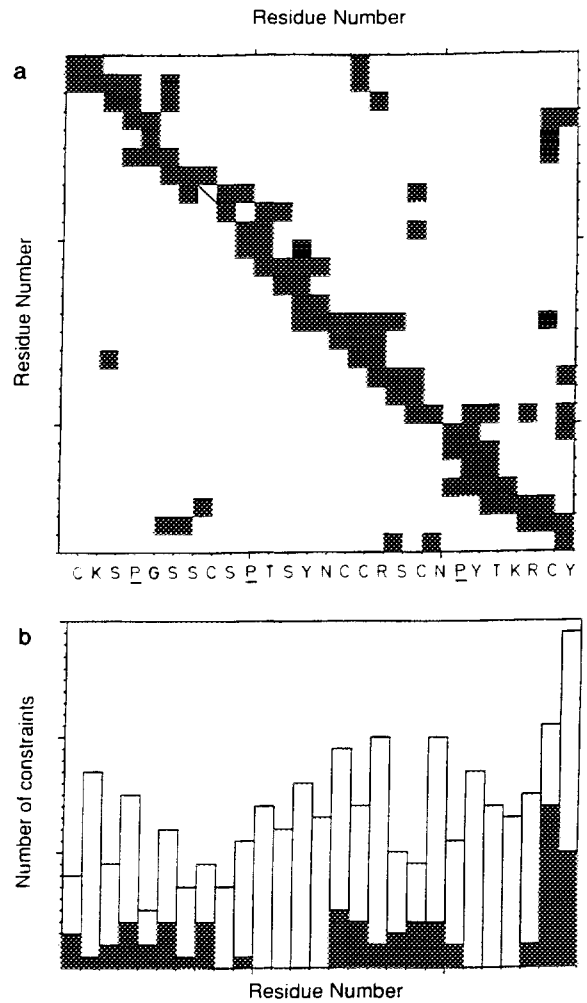

Figure 2. Distribution of distance restraints. a) Spatial. The triangle below the diagonal indicates backbone-backbone proton connectivities; the upper triangle indicates the rest. b) Sequential. Filled bars represent long-range restraints ($|i-j| > 4$) ; open bars represent short-range restraints.

as input for the GLOMSA program. The $C^{\beta}H$ protons of Hyp-4, Cys-8, Hyp-10, Cys-15, Asn-20, Hyp-21, Cys-26, Tyr-27, and also the CONHZ and CONHE protons of the terminal carboxamide group were stereospecifically assigned. A final improved set of structures were then calculated which satisfied the distance restraints with no violation greater than 0.32 Å and which, upon restrained energy minimization, showed good covalent geometry and non-bonded contacts. The potential energy of the energy-minimized mean atomic structure was -835.2 KJ mol^{-1}, with a contribution from the Lennard-Jones term of -459.9 KJ mol^{-1}, and only 12.3 KJ mol^{-1} arising from the NOE distance restraints.

The mean RMSD between each of the 8 structures and the mean atomic coordinates for all residues is 0.82 ± 0.06 Å for the backbone atoms. When the least defined regions (residues 1, 10-13, and 21-24) are not taken into account this value goes down to 0.54 ± 0.05 Å (Table 2). A plot of the mean

Table 2. Cartesian coordinate RMSD (Å) for 8 ω-CgTx structures

	residues 1-27	residues 2-9 ,14-20 ,25-27
backbone:		
mean pairwise RMSD	1.18±0.18	0.77±0.11
mean RMSD of 8 structures *versus* mean atomic coordinates	0.82±0.06	0.54±0.05
all non-H atoms:		
mean pairwise RMSD	2.10±0.29	1.74±0.35
mean RMSD of 8 structures *versus* mean atomic coordinates	1.45±0.18	1.22±0.25

pairwise backbone RMSD per residue number for the best 8 structures and the mean atomic coordinates is shown in Figure 3. Figure 4 shows the fit of the backbone of all structures.

DISCUSSION

The three disulfide bridges constrain the ω-CgTx backbone and help stabilize the overall compact globular folding of the peptide. Two of these S-S linkages are buried (S8-S19 and S15-S26) whereas the S1-S16 cross-link near the amino terminus is part of an external loop. The four hypervariable

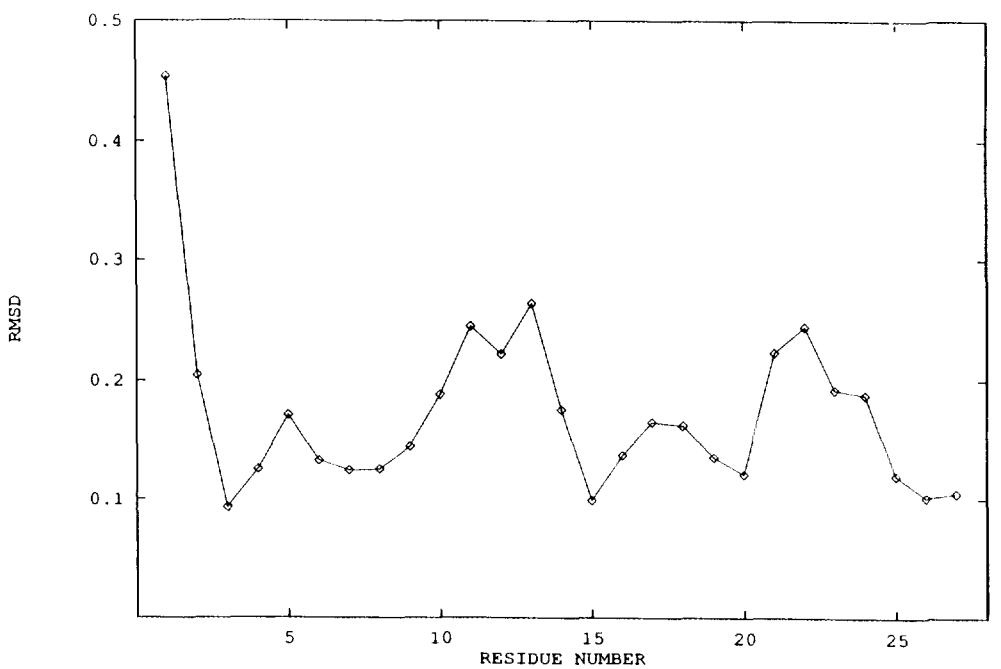

Figure 3. Plot of the mean pairwise backbone RMSD (in Å) per residue number, for the best 8 structures and the mean atomic coordinates.

Figure 4. Best-fit superposition for the backbone of the final set of structures with respect to the mean atomic coordinates.

regions between the Cys residues give rise to different secondary structure arrangements: i) a type II β-turn involving the highly conserved Gly-5 and stabilized by a hydrogen bond between CO(Ser-3) and HN(Ser-6), ii) a type I β-turn stabilized by a hydrogen bond between CO(Ser-9) and HN(Ser-12), iii) part of a loop comprising residues 15-18 (Arg-17 and Ser-18), and iv) an incipient α-helix involving a 1-4 hydrogen bond between CO(Asn-20) and HN(Lys-24). The backbone of the second and the fourth of these segments is the least defined in the molecule. The absence of cross peaks for this region in the NOESY spectra (Figure 2) can be attributed to a large mobility of these loops. On the other hand, the side chains of Lys-2, Ser-6, Cys-8, Cys-15, Cys-16, Cys-19, Asn-20, Tyr-22, Thr-23, Lys-24, Cys-26, and Tyr-27 are better defined than the rest.

Additional main chain hydrogen bonds are found between CO(Ser-6) and HN(Cys-26), CO(Ser-18) and HN(Tyr-27), CO(Arg-25) and HN(Asn-20), and CO(Cys-26) and HN(Gly-5). The side chains of Lys-2 and Lys-24 emerge radially from the peptide core and are located on opposite faces of the structure. The same is true for the side chains of Arg-17 and Arg-25 whereas the phenol rings of the three Tyr residues are found on a plane at the same face of the molecule (Figure 5). The side chain of Asn-20 is firmly fixed by two hydrogen bonds, one between Oγ(Thr-23) and $N^{\delta}H2$(Asn-20) and another one between Oδ(Asn-20) and HN(Tyr-22).

The peptide bond of Hyp-21 is clearly *trans* in the final 8 structures but the conformations of Hyp-4 and Hyp-10 are less well defined. A total of 14 hydroxyl groups are found at the periphery fully exposed to the solvent, and account for the extremely good solubility of this peptide in water. Two of them appear to be involved in intramolecular hydrogen bonds, namely, HOγ(Ser-3) and HOγ(Ser-18), which hydrogen bond to the carbonyl oxygens of Tyr-27 and Arg-17, respectively, and four others (Oγ(Ser-9), OD1(Hyp-10), Oγ(Thr-11) and Oγ(Ser-12)) define the corners of an imaginary trapezoid in the vicinity of Tyr-13.

All of these features provide different combinations of patterns for intermolecular recognition. In common with other ion channel proteins, anionic sites complementary to the positively charged side

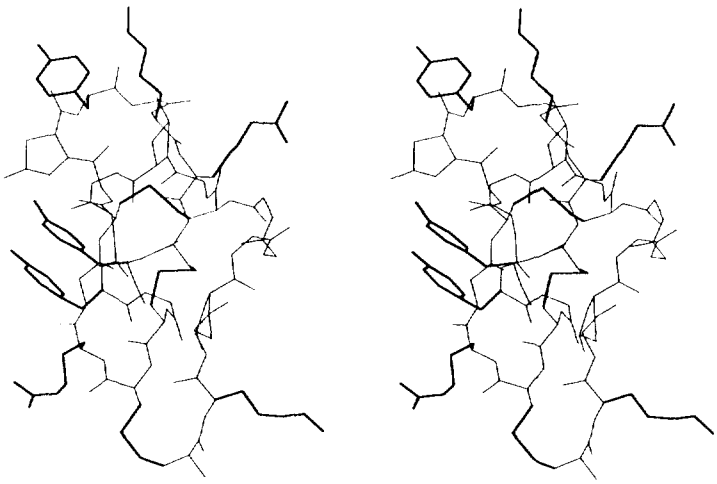

Figure 5. Stereoview of the energy-minimized mean atomic structure of ω-CgTx. The side chains of Cys, Tyr, Arg and Lys are highlighted. For all other residues, except for hydroxyprolines, only the backbone atoms are displayed.

chains of ω-CgTx are expected to be located in the extracellular "funnel" part of the channel. In this respect, the recent cloning and sequencing (18) of an ω-CgTx-sensitive human N-type calcium channel provide a foundation for further studies of this interaction at the molecular level.

ACKNOWLEDGMENTS. This work has been partially supported by grants PB-91-0368, PB-91-022-C02-01 and PM-92-0039 from the Spanish DGICYT.

REFERENCES

1. Cruz, L.J.; Gray, W.R.; Yoshikami, D.; Olivelra, B.M. (1985) *J.Toxicol.-Toxin Rev.* 4, 107-132.
2. Oliveira, B.M.; Rivier, J.; Scott, J.K.; Hillyard, D.R.; Cruz, L.J. (1991) *J.Biol.Chem.* 266, 22067-22070.
3. Kerr, L.M.; Yoshikami, D. *Nature* (1984) 308, 282-284.
4. Sher, E.; Clementi, F. *Neurosci.* (1991) 42, 301-307.
5. Kobayashi, Y.; Ohkubo, T.; Kyogoku, Y.; Nishiuchi, Y.; Sakakibara, S.; Braun, W.; Go, N. (1989) *Biochem.* 28, 4853-4860.
6. Pardi, A.; Galdes, A.; Florance, J.; Maniconte, D. (1989) *Biochem.* 28, 5494-5501.
7. Ott, K.H.; Becker, S.; Gordon, R.D.; Rüterjans, H. (1991) *FEBS Lett.* 278, 160-166.
8. Lancelin, J.M.; Kohda, D.; Tate, S.; Yanagawa, Y.; Abe, T.; Satake, M.; Inagaki, F. (1991) *Biochem.* 30, 6908-6916.
9. Aue, W.P.; Bartholdi, E.; Ernst, R.R. (1976) *J.Chem.Phys.* 64, 2229-2246.
10. Bax, A.; Davis, D.G. (1985) *J.Magn.Reson.* 65, 393-402.
11. Macura, S.; Ernst, R.R. (1980) *Mol.Phys.* 41, 95-117.
12. Bolens, R.; Vuister, G.W.; Kleywegt, G.J.; Koning, M.M.G.; Rullman, J.A.C. (1990) Triton Software Manual, Department of Chemistry, University of Utrech, The Netherlands.
13. Wüthrich, K.; Billeter, M.; Braun, W. (1983) *J.Mol.Biol.* 169, 949-961.
14. Güntert, P.; Braun, W.; Wüthrich, K. (1991) *J.Mol.Biol.* 217, 517-530.
15. Van Gunsteren, W.F.; Berendsen, H.J.C. (1987) Groningen Molecular Simulation (GROMOS) Library Manual, Biomos, Groningen, The Netherlands.
16. McLachlan, A.D. (1979) *J.Mol.Biol.* 128, 49-79.
17. Wüthrich, K. (1976) *NMR of Proteins and Nucleic Acids*, John Wiley , New York.
18. Williams, M.E.; Brust, P.F.; Feldman, D.H.; Patthi, S.; Simerson, S.; Maroufi, A.; McCue, A.F.; Veliçelebi, G.; Ellis, S.B.; Harpold, M.M. (1992) *Science* 257, 389-395.